Structural and Magnetic Characterization of Mixed Oxides: A Study of Li-Ni-O and Li-Mn-O Systems

V. Massarotti, D. Capsoni, M. Bini, C. B. Azzoni[a], M. C. Mozzati[a], and A. Paleari[b]

Department of Physical Chemistry of the University and CSTE-CNR,
Viale Taramelli 16, I-27100 Pavia
[a] INFM Department of Physics "A. Volta" of the University, Via Bassi 6, I-27100 Pavia
[b] INFM Department of Materials Science of the University, Via Emanueli 15, I-20126 Milano

The present paper details the way to determine the cation distribution in mixed oxides with transition ions from the diffraction and magnetic susceptibility data. This approach allows one to determine phase abundances and phase compositions by two combined procedures. By X-ray diffraction Rietveld profile refinement and magnetic susceptibility data analysis it is possible to estimate the ratio and the occupancy factor of paramagnetic ions in different oxidation states. A brief discussion of practical cases is reported. In the Li-Ni-O system the lithium cationic fraction of the ordered phase $Li_{2x}Ni_{2-2x}O_2$ increases monotonically with the total lithium fraction x_t for $0.31 \leq x_t \leq 0.46$. In the Li-Mn-O system for $0.36 \leq x_t \leq 0.53$ the Li_2MnO_3 fraction has been determined, and for the coexistent $Li[Li_yMn_{2-y}]O_4$ spinel phase the dependence of y on x_t has been evaluated.

Key words: X-ray Powder Diffraction; Magnetic Susceptibility; Lithium Nickel Oxides; Lithium Manganese Oxides; Lithium Manganese Spinel.

1. Introduction

The principal aim of material science is to plan compounds with predetermined characteristics, through the knowledge of the relationships between composition, structure and properties.

Ternary Li-M-O systems with lithium and transition metal cations often possess a wide homogeneity range and properties markedly dependent on the effective cationic composition and on the valence state of the transition cation [1–3]. In fact, large variations of structural [1, 4–6], microstructural [7, 8], magnetic [1, 9] and transport properties [10] are sometimes observed in these systems as functions of the composition. As a result, such compounds can be considered useful systems for the understanding of the process of charge transfer and magnetic interactions in crystalline solids and may suggests interesting applications for devices with composition-tunable properties. In particular, the layered rock-salt $LiMO_2$ structure (M = V, Cr, Mn, Co, Ni) (2-D array of edge-sharing MO_6 and LiO_6 octahedra) and the oxygen close packed spinel type $LiMn_2O_4$ structures (3-D array of edge-sharing MnO_6 octahedra and LiO_4 tetrahedra)

can both sustain the reversible extraction/insertion of lithium [2, 11–13]. Thus, they are potential candidates as electrode materials for a light and rechargeable battery known as "rocking-chair" system [14, 15]. Mixed lithium-nickel, lithium-cobalt and lithium-manganese oxides have recently been used for the preparation of cathode materials for rechargeable lithium-batteries [16–18] and as selective hydrocarbon oxidation catalysts [19]. In both cases the properties are due to the coexistence, of the transition cations in two different oxidation states and to the cation incoporation into the crystal sites.

An important goal in this case is it therefore to know the cation distribution in order to obtain a structural model as a function of the composition and possibly of the synthesis conditions. Useful physical observables for this aim are the structure factors of the reflections (nuclear and magnetic), contributing to the diffraction patterns of X-rays and neutrons, and the temperature dependence of the magnetic susceptibility arising from the magnetic moments of the different valence states of the transition cations.

We will show how XRD and paramagnetic susceptibility measurements can be effective to determine the abundance and composition of the phases. In this way the stoichiometry of the components of the system, generally dependent on the bulk composition, preparation temperature and oxygen partial pressure, can be obtained.

2. Experimental Details

2.1. Materials and Sample Preparation

Li-Ni-O system: the samples were prepared from the reactive system Aldrich (99.99%) NiO/Carlo Erba (R.P.) Li_2CO_3, the starting mixture having the lithium cationic fraction, x_t, ranging between 0.31 and 0.46. The reagents were intimately mixed by grinding in an agate mortar and then heated at 5 K/min up to 1073 K in alumina crucibles. An isothermal step was then held for an annealing time of 8 h at this temperature, followed by cooling down to room temperature at 5 K/min.

Li-Mn-O system: the samples were prepared by the reactive system Alfa (99.9%) MnO/Carlo Erba (R.P.) Li_2CO_3 from a starting mixtures with $0.33 < x_t < 0.53$. Heating and cooling cycles were the same as in the previous case.

2.2. Apparatus and Procedures

Diffraction data were obtained by a Philips PW1710 powder diffractometer equipped with a Philips PW1050 vertical goniometer. Use was made of the CuK_α radiation ($K_{\alpha1} = 1.54056$ Å; $K_{\alpha2} = 1.5443$ Å), selected by means of a graphite monochromator. Patterns were collected in the angular range $15° < 2\theta < 130°$ in step scan mode (step width 0.03° or 0.025°; counting time 10 s/step or 1 s/step).

Structural and profile parameters were obtained by the Rietveld refinement procedure [20] performed with the program WYRIET version 3.5 [21, 22].

Static magnetic susceptibility measurements were carried out from 300 K down to liquid helium temperature at a magnetic field of 200 mT by using a Faraday balance susceptometer with a sensitivity of 0.1 µg and a continuous-flow cryogenic apparatus. For experimental details see [9, 10].

3. Fundamentals of an XRD and Static Susceptibility Approach

3.1. X-Ray Diffraction

The XRD pattern simulation can be performed on the basis of the Rietveld method [20] with the program WYRIET version 3.5 [21, 22] for multiphase analysis. The residual M is minimized,

$$M = \sum w_i (y_{o,i} - y_{c,i})^2 \tag{1}$$

where $y_{o,i}$ is the observed intensity at each point i of the pattern; w_i the statistical weight of each observation and $y_{c,i}$ the total intensity calculated at point i. For the general case of multiphase systems, $y_{c,i}$ can be expressed by the formula

$$y_{c,i} = \sum K_p \sum m_{h,p} L_{h,p} |F_{h,p}|^2 G_{h,p,i} A_{h,p,i} + y_{b,i} \tag{2}$$

where K_p is the scale factor, $m_{h,p}$ the multiplicity of the reflection, $L_{h,p}$ the Lorentz-polarization factor, $F_{h,p}$ the structure factor, $G_{h,p,i}$ the peak profile function (Pseudo-Voigt or Pearson VII) [21, 22], $A_{h,p,i}$ the peak asymmetry function and $y_{b,i}$ the background intensity contribution. In (2) all the h reflection contributions of each p phase are considered. The above procedure had previously been used to determine the relative amounts of phases such as ordered and disordered solid solutions and stoichiometric compounds, as well as the cation occupancy factors, in the systems Li-Ni-O [1, 23] and Li-Mn-O [7, 24].

3.2. Magnetic Susceptibility

The magnetic behaviour of a transition metal mixed oxide at sufficiently high temperature approaches the Curie-Weiss (C-W) law independently of the specific magnetic order that the structure can sustain at low temperature, as one can see from the high temperature asymptotic mean field expression for magnetic oxides. So, in the high temperature range the paramagnetic mass susceptibility χ_m depends on the temperature T according to the equation

$$\frac{1}{\chi_m} = \frac{T - \theta}{C_m}, \tag{3}$$

where θ is the Weiss constant and C_m the Curie constant referred to the mass unity. θ is related to the local interaction sign and gives information about the magnetically ordered phases (if existing). C_m is related to the magnetic moment of the considered ion and thus to the mean effective number of Bohr magnetons, m, per ion. Through the relation

$$m^2 = \frac{3k_B}{N_A \mu_B^2} \cdot \frac{WC_m}{n}, \tag{4}$$

where W is the weighted average of the component molar mass of the sample, n the number of magnetic ions per unit formula, k_B the Boltzmann constant, N_A Avogadro's number, μ_B the Bohr magneton, and m depends on the mean valence state of the magnetic ions and

is directly related to the phase abundance of the system and to the composition of each phase, it is possible to determine the compositional parameters.

4. Comparison with the Experiment

4.1. Li-Ni-O System

For $x_t < 0.32$ the simple solid solution $Li_xNi_{1-x}O$ (SSS) and the ordered solid solution $Li_{2x}Ni_{2-2x}O_2$ (OSS) are both present [9, 23], and the paramagnetic region is observable at temperatures remarkably higher than covered in this work (see Fig. 1, curve a). The SSS contribution to the slope of $1/\chi_m$ is negligible since it is nearly independent of the temperature. Therefore, the fraction (α) of OSS in the sample must be deduced from the Rietveld refinement results, while the C-W parameters are obtained from the paramagnetic range of the $1/\chi_m$ vs. T curve. Then it is possible to determine the lithium content x_{OSS} in the OSS phase of the mixture by considering the relations of x_{OSS} with W, n and m^2:

$$W = 2\alpha[x_{OSS}A_{Li} + (1 - x_{OSS})A_{Ni} + A_O], \quad (5)$$

where only the contribution of the OSS phase has been considered because it represents the only contribution to the T dependence of $1/\chi_m$, and A_{Li}, A_{Ni} and A_O are the atomic mass of Li, Ni, and O,

$$n = 2 - 2x_{OSS}, \quad (6)$$

$$m^2 = \frac{(1 - 2x_{OSS})m^2_{Ni^{2+}}}{1 - x_{OSS}} + \frac{x_{OSS}m^2_{Ni^{3+}}}{1 - x_{OSS}}. \quad (7)$$

Inserting (5)–(7) in (4), the x_{OSS} value can be obtained from the value of C_m determined by (3). In Fig. 1 we report (curve a) the $1/\chi_m$ data of our $x_t = 0.31$ sample for $100\ K < T < 300\ K$, compared with literature data [25] for $300\ K < T < 600\ K$. The two sets of data agree near room temperature.

In the range $x_t > 0.32$, only the OSS phase is present [4, 9, 23] and the paramagnetic region is observable at relatively low temperature [9]: the parameters θ and C_m of (3) can easily be obtained from the same equation. Figure 1, curve b, shows the trend of $1/\chi_m$ as a function of

Fig. 2. System Li-Ni-O: x_t dependence of (a) OSS phase fraction α determined by XRD and (b) lithium content of the OSS phase determined by XRD ($\circ$) and by susceptibility ($\square$) measurements.
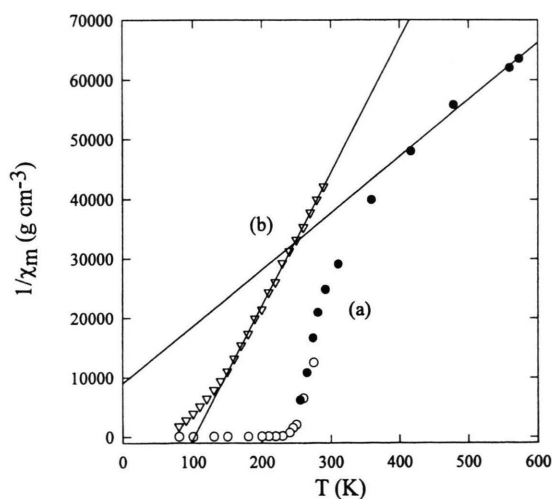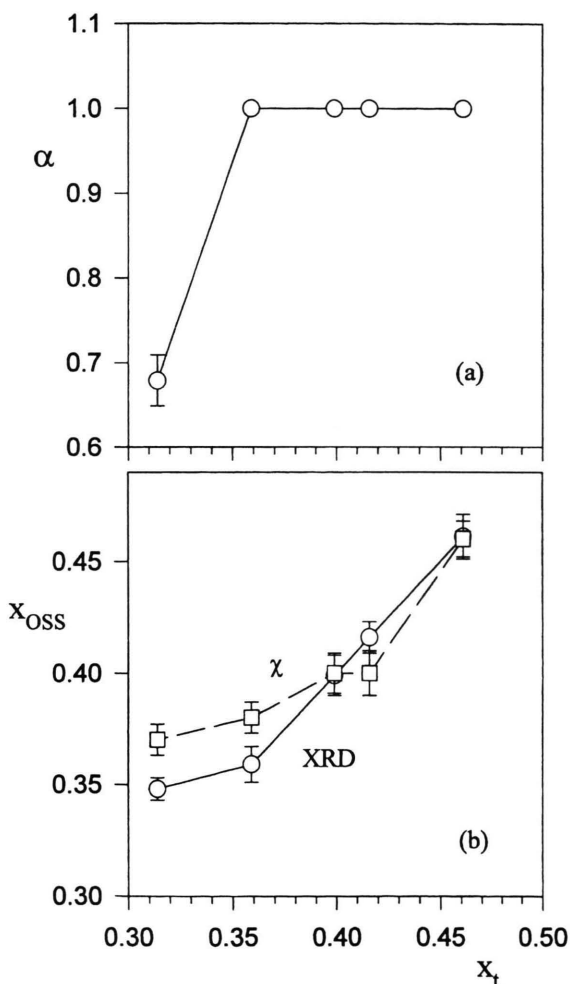
Fig. 1. System Li-Ni-O: $1/\chi_m$ values as functions of T for (a) $x_t = 0.31$ and (b) $x_t = 0.46$: present ($\circ$) and literature data ($\bullet$) are compared. Regression lines for the paramagnetic range are shown.
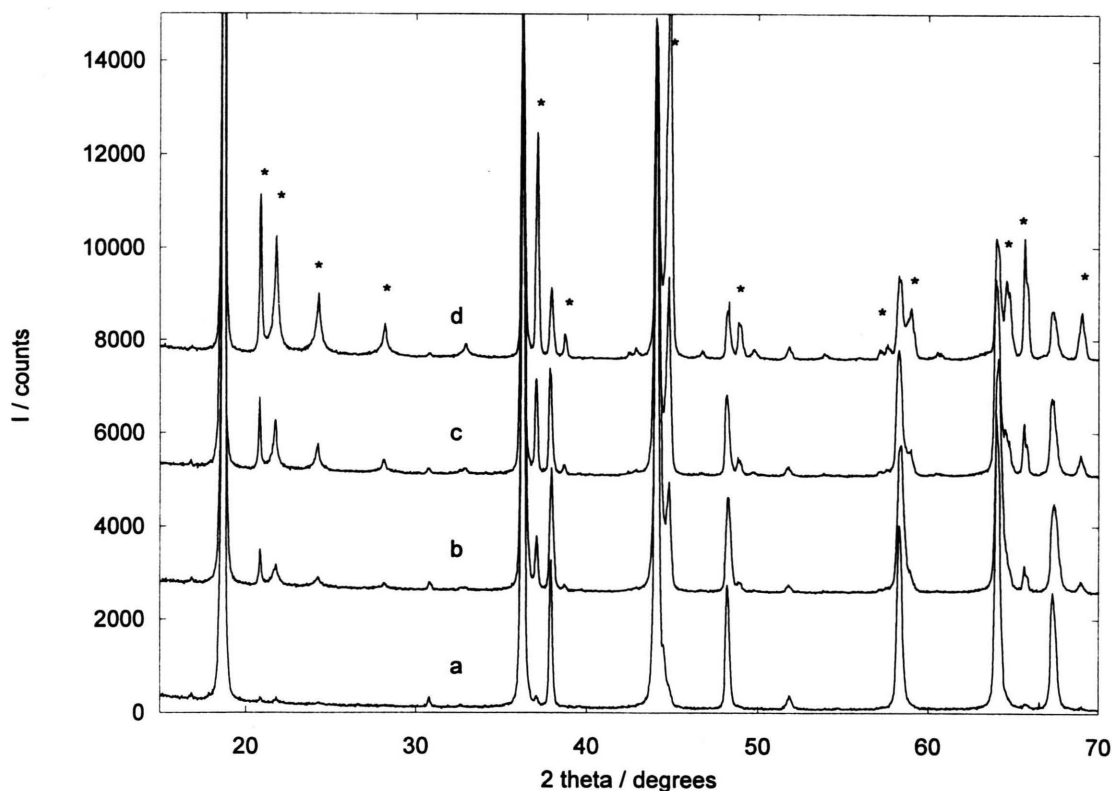
Fig. 3. System Li-Mn-O: comparison between the patterns of lithium manganese oxide samples with $x_t = 0.36$ (a), $x_t = 0.40$ (b), $x_t = 0.44$ (c) and $x_t = 0.53$ (d). The stars mark the most intense peaks of the Li_2MnO_3 phase.

T for the $x_t = 0.46$ sample. The lithium content of the OSS phase (x_{OSS}) can be determined both by the refinement of the cation sites occupancy factor and by solving (4) as a function of x_{OSS}.

The above procedures have been used to obtain the pertinent Li-content of the OSS phase fraction (see Fig. 2a) for the samples in the composition range $0.31 < x_t < 0.46$. The results are reported in Fig. 2b and compared with the values estimated by XRD Rietveld analysis.

4.2. Li-Mn-O System

In the Li-Mn-O system the detected crystallographic phases are $LiMn_2O_4$, spinel type, and Li_2MnO_3, monoclinic rock-salt type. As an example, in Fig. 3 the XRD patterns of some samples are reported to show the increase in the Li_2MnO_3 abundance with increasing x_t (the stars refers to literature Li_2MnO_3 data).

As reported in previous papers [7, 24] a suitable profile fit on the spinel phase peaks can be obtained, for $x_t > 0.35$ samples, on considering an additional diffraction component close to the spinel peaks. That was attributed to the presence of a Li-rich spinel form coexisting at room temperature with the stoichiometric one. The two forms differ both in cell dimensions and composition. To obtain the best result in the Rietveld profile analysis it was necessary to model the rock-salt type Li_2MnO_3 phase and two limiting spinel forms, one stoichiometric (larger cell) and another Li-enriched. Figure 4 shows, as an example, the Rietveld refinement results for the $x_t = 0.40$ sample. From the Rietveld procedure the phase abundances and Li content in each sample were obtained, and those pertinent to the two spinel forms were used to evaluate the mean spinel phase composition; the averaged formula may be expressed by $Li[Li_yMn_{2-y}]O_4$.

The y values can also be obtained from susceptibility data, related to the mean sample composition and then to the mean valence state of the transition cation, following the procedure previously outlined. The $1/\chi_m$ vs. T curves for the samples with $x_t = 0.36, 0.40, 0.44$ and 0.53 are reported in Figure 5.
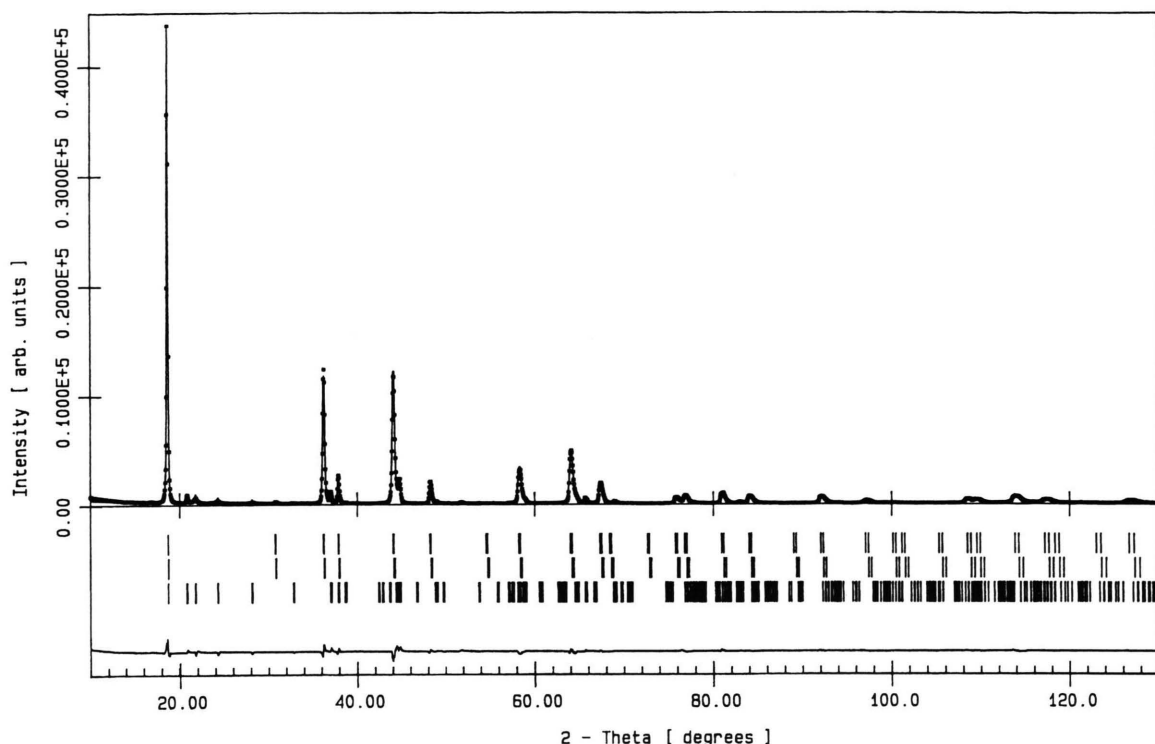
Fig. 4. System Li-Mn-O: comparison between the observed (dots) and calculated (solid line) pattern obtained after Rietveld refinement for the $x_t = 0.40$ sample. In the lower part, the difference curve is plotted and bars for the reflection positions are shown.

To describe the suceptibility data it was necessary to take into account the two distinct phases $Li_{1+y}Mn_{2-y}O_4$ and Li_2MnO_3, for which the weight fractions α and β, respectively, are considered. The Li_2MnO_3 fraction $\beta = (1 - \alpha)$ can be obtained by both XRD and, more reliably, by EPR determination [24] (in general, when no EPR signal is available, other techniques, for example density determinations, must be used), and the following equations for the molar mass (W), the number of magnetic cations (n) and the effective number of Bohr magnetons (m) are used:

$$W = \alpha[(1 + y)A_{Li} + (2 - y)A_{Mn} + 4A_O] \qquad (8)$$
$$+ (1 - \alpha)W_{Li_2MnO_3},$$

where A_{Mn} is the atomic mass of Mn and $W_{Li_2MnO_3}$ the molar mass of Li_2MnO_3,

$$n = \alpha(2 - y) + (1 - \alpha) \qquad (9)$$

and

$$m^2 = \alpha\left(\frac{1 - 3y}{2 - y}m^2_{Mn^{3+}} + \frac{2y + 1}{2 - y}m^2_{Mn^{4+}}\right) \qquad (10)$$
$$+ (1 - \alpha)m^2_{Mn^{4+}}.$$
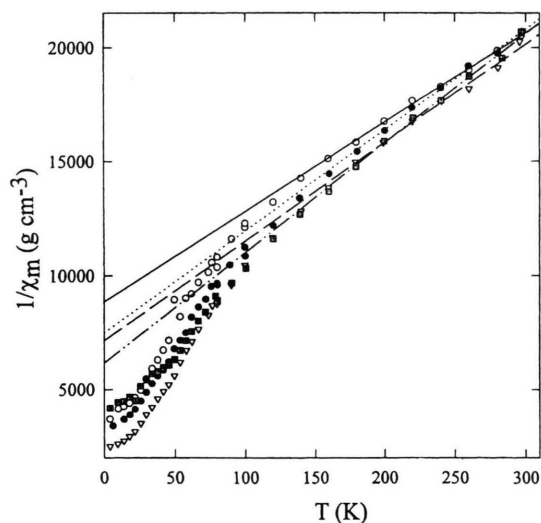
Fig. 5. System Li-Mn-O: $1/\chi_m$ values as functions of T for $x_t = 0.36$ ($\circ$), $x_t = 0.40$ ($\triangledown$), $x_t = 0.44$ ($\bullet$) and $x_t = 0.53$ ($\blacksquare$). Regression lines in the paramagnetic range region are shown.

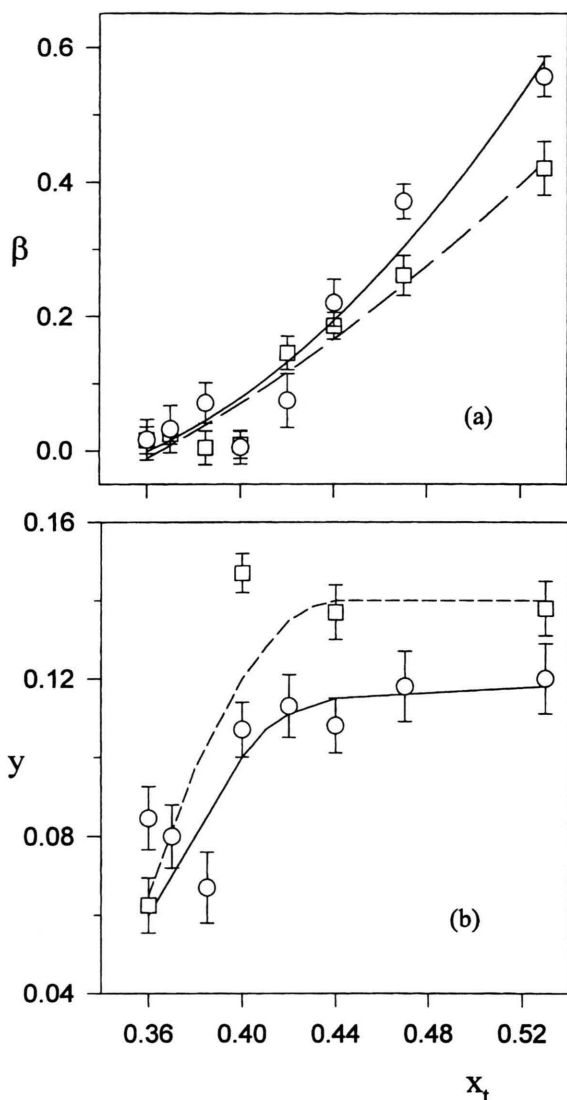Inserting (8)–(10) in (4), the y value can be obtained upon C_m determination from (3). The results obtained are reported in Figure 6. The values of the weight fraction β (Fig. 6a) and the deviation from stoichiometry (Fig. 6b), deduced by Rietveld refinement and by magnetic measurements, are compared. The sensible overestimation of the XRD β values with respect to the EPR ones, for $x > 0.44$ (Fig. 6a), causes a corresponding underestimation of the y XRD values, as can be seen in Figure 6b. As previously discussed [23], the overestimation of β by Rietveld determination can be due to the influence of the microstructure of the phases.

5. Conclusions

The comparison between the analysis of the paramagnetic response and the Rietveld refinement of diffraction data allowed us to evaluate the stoichiometry deviation in ternary oxides and to relate the composition of the system to other physical properties. In effect, knowledge of the mean valence state of the transition cations and the abundances of the different phases, together with structural information represents a suitable tool for the determination of property-composition relations.

In the case of substitutional solid solutions in the systems Li-Ni-O and Li-Mn-O we established a correlation between the magnetic properties and the mean valence state of the transition cations in the component phases as a function of lithium substitution. Other important aspects concern the influence of preparation conditions on the mean valence state, as reported in a recent paper on the Li-Mn-O system [26], where the spinel phase was considered together with compounds displaying other stoichiometry and transition cation valence states.

[1] J. B. Goodenough, D. G. Wickham, and W. J. Croft, J. Phys. Chem. Solids **5**, 107 (1958).
[2] G. Dutta, A. Manthiram, J. B. Goodenough, and J.-C. Grenier, J. Solid State Chem. **96**, 123 (1992).
[3] B. Gillot, J. L. Baudour, F. Bouree, R. Metz, R. Legros, and A. Rousset, Solid State Ionics **58**, 155 (1992).
[4] W. Li, J. N. Reimers, and J. R. Dahn, Phys. Rev. B **46**, 3236 (1992).
[5] W. Li, J. N. Reimers, and J. R. Dahn, Phys. Rev. B **49**, 826 (1994).
[6] W. I. F. David, M. M. Thackeray, L. A. De Picciotto, and J. B. Goodenough, J. Solid State Chem. **67**, 316 (1987).
[7] V. Massarotti, M. Bini, and D. Capsoni, Z. Naturforsch. **51a**, 267 (1996).
[8] V. Massarotti, M. Bini, D. Capsoni, P. Scardi, and M. Leoni, Mat. Sci. Forum in the press.
[9] C. B. Azzoni, A. Paleari, V. Massarotti, M. Bini, and D. Capsoni, Phys. Rev. B **53**, 703 (1996).
[10] V. Massarotti, D. Capsoni, M. Bini, G. Chiodelli, C. B. Azzoni, M. C. Mozzati, and A. Paleari, J. Solid State Chem. **131**, 94 (1997).

[11] J. B. Goodenough, M. M. Thackeray, W. I. F. David, and P. G. Bruce, Rev. Chimie Minerale **21**, 435 (1984).

[12] G. Pistoia, G. Wang, and C. Wang, Solid State Ionics **58**, 285 (1992).

[13] M. S. Whittingham, R. Chen, T. Chirayil, and P. Zavalij, Solid State Ionics **94**, 227 (1997).

[14] J. M. Tarascon and D. Guyomard, Electrochim. Acta **38**, 1221 (1993).

[15] P. G. Bruce, Phil. Trans. Roy. Soc. Lond. A **354**, 1577 (1996).

[16] T. Ohzuku, A. Ueda, and M. Nagayama, J. Electrochem. Soc. **140**, 1862 (1993).

[17] M. M. Thackeray, A. de Kock, M. H. Rossouw, D. Liles, R. Bittihn, and D. Hoge, J. Electrochem. Soc. **139**, 363 (1992).

[18] F. K. Shokoohi, J. M. Tarascon, B. J. Wilkens, D. Guyomard, and C. C. Chang, J. Electrochem. Soc. **139**, 1845 (1992).

[19] M. Hatano and K. Otsuka, J. Chem. Soc., Faraday Trans. **85**, 199 (1989).

[20] H. M. Rietveld, J. Appl. Cryst. **2**, 65 (1969).

[21] J. Schneider, Proceeding IUCR Int. Workshop on the Rietveld Method, Petten 1989.

[22] D. B. Wiles and R. A. Young, J. Appl. Cryst. **14**, 149 (1981).

[23] V. Massarotti, D. Capsoni, and M. Bini, Z. Naturforsch. **50a**, 155 (1995).

[24] V. Massarotti, D. Capsoni, M. Bini, C. B. Azzoni, and A. Paleari, J. Solid State Chem. **128**, 80 (1997).

[25] W. Bronger, H. Bade, and W. Klemm, Z. Anorg. Allg. Chemie **333**, 188 (1964).

[26] C. Masquelier, M. Tabuchi, K. Ado, R. Kanno, Y. Kobayashi, Y. Macki, O. Nakamura, and J. B. Goodeneough, J. Solid State Chem. **123**, 255 (1996).